

RESEARCH ARTICLE

Transgenic zebrafish models reveal distinct molecular mechanisms for cataract-linked α A-crystallin mutants

Shu-Yu Wu , Ping Zou, Sanjay Mishra , Hassane S. Mchaourab*

Department of Molecular Physiology and Biophysics, Vanderbilt University, Nashville, TN, United States of America

* hassane.mchaourab@Vanderbilt.Edu



Abstract

Mutations in the small heat shock proteins α -crystallins have been linked to autosomal dominant cataracts in humans. Extensive studies *in vitro* have revealed a spectrum of alterations to the structure and function of these proteins including shifts in the size of the oligomer, modulation of subunit exchange and modification of their affinity to client proteins. Although mouse models of these mutants were instrumental in identifying changes in cellular proliferation and lens development, a direct comparative analysis of their effects on lens proteostasis has not been performed. Here, we have transgenically expressed cataract-linked mutants of α A- and α B-crystallin in the zebrafish lens to dissect the underlying molecular changes that contribute to the loss of lens optical properties. Zebrafish lines expressing these mutants displayed a range of morphological lens defects. Phenotype penetrance and severity were dependent on the mutation even in fish lines lacking endogenous α -crystallin. The mechanistic origins of these differences were investigated by the transgenic co-expression of a destabilized human γ D-crystallin mutant. We found that the R49C but not the R116C mutant of α A-crystallin drove aggregation of γ D-crystallin, although both mutants have similar affinity to client proteins *in vitro*. Our working model attributes these differences to the propensity of R49C, located in the buried N-terminal domain of α A-crystallin, to disulfide crosslinking as previously demonstrated *in vitro*. Our findings complement and extend previous work in mouse models and emphasize the need of investigating chaperone/client protein interactions in appropriate cellular context.

OPEN ACCESS

Citation: Wu S-Y, Zou P, Mishra S, Mchaourab HS (2018) Transgenic zebrafish models reveal distinct molecular mechanisms for cataract-linked α A-crystallin mutants. PLoS ONE 13(11): e0207540. <https://doi.org/10.1371/journal.pone.0207540>

Editor: Yong-Bin Yan, Tsinghua University School of Life Sciences, CHINA

Received: July 16, 2018

Accepted: November 1, 2018

Published: November 26, 2018

Copyright: © 2018 Wu et al. This is an open access article distributed under the terms of the [Creative Commons Attribution License](https://creativecommons.org/licenses/by/4.0/), which permits unrestricted use, distribution, and reproduction in any medium, provided the original author and source are credited.

Data Availability Statement: All relevant data are within the paper.

Funding: This work has been funded by National Eye Institute (<https://nei.nih.gov/>), R01 EY12018 and P30 EY008126 to HSM.

Competing interests: The authors have declared that no competing interests exist.

Introduction

In its most common form, age-related cataract is an opacity of the lens characterized by the formation of protein aggregates that scatter light [1]. Protein aggregation is driven by the progressive insolubilization of lens proteins as a consequence of age-dependent changes to their sequences and structures [2, 3]. Terminally differentiated lens fiber cells, devoid of cellular machineries that repair and turn proteins over, rely on two small heat shock proteins (sHSPs), α A- and α B-crystallin, which function as molecular chaperones by sequestering thermodynamically destabilized

client proteins to inhibit aggregation [2–5]. The prevailing model of age-related cataract posits that the chaperone capacity of α -crystallins is titrated out by binding of damaged lens proteins as well as truncation and insolubilization of the sHSPs themselves [6–8]. Detailed models of stable and transient interactions with model client proteins revealed activation mechanisms of α -crystallins and defined the energetics of the chaperone interactions [9–17].

Consistent with a central role in lens development and transparency, point mutants of α -crystallins have been associated with hereditary cataracts [5, 18]. Multiple studies dissected how the mutations affect the interactions with client proteins *in vitro* [19–22]. Koteiche and Mchaourab demonstrated that two α A-crystallin substitutions, R49C and R116C, lead to a 100-fold increase in the affinity to the client protein T4 lysozyme (T4L) [11]. Interpreted in the framework of a model where the affinity of the chaperone is thermodynamically coupled to the folding equilibrium of T4L, these findings supported the conclusion that the mutants can behave as “unfoldases” [23]. The mutated chaperones are predicted to bind undamaged proteins, which promotes their unfolding, and consequently leads to saturation of the chaperone binding sites and the formation of large chaperone/protein aggregates [23]. A similar conclusion was reached for the α B-crystallin R120G, a human mutation which has been associated with cardiomyopathy [20].

Mouse models of α A- and α B-crystallin mutants associated with hereditary cataract delineated a number of important cellular changes and shed light on previously unappreciated physiological roles for these proteins in apoptosis and genomic maintenance [24–27]. However, due to inherent limitations of the mouse model, a direct analysis of how modification of chaperone/client protein interactions affects lens proteostasis is not straightforward. Studies of the knock-in model of α A-R49C suggested changes in these interactions as well as in the level of insolubilization of lens proteins [26]. However, the former was only observed in the heterozygotes, which paradoxically had a moderate cataract phenotype. Thus, while these preliminary observations are consistent with the model of Koteiche and Mchaourab [11], a more detailed interrogation of these interactions in the lens is needed.

To establish a link between *in vitro* mechanistic models of α -crystallin chaperone function and their roles in lens aging, we have utilized zebrafish (*Danio rerio*) as an experimental model organism. A number of advantages makes zebrafish ideal for such an endeavor including ease and cost of rearing the animals and the size of the embryo clutches [28, 29]. Moreover, the transparency of the embryos during the first few days of their development and their relatively large eyes, which are functional at 3 days post fertilization (dpf), enable the examination of lens gross morphology by bright field microscopy [30–34]. The structure and function of the zebrafish adult lens parallel those of the mature human lens with respect to symmetry, refraction, transparency and optical function [29, 35, 36]. Previous work from our laboratory demonstrated that both α -crystallins are required for lens development [32, 37]. Furthermore, we established the utility of the zebrafish as a model for lens proteostasis by demonstrating a correlation between the level of major lens defects and the expression of progressively destabilized mutants of human γ D-crystallin [33].

Here, we transgenically expressed two mutants of α A-crystallins associated with hereditary cataract and the cardiomyopathy-linked R120G mutant of α B-crystallin in the zebrafish lens. In addition to characterizing the phenotypes of the transgenic lines, we challenged the proteostasis network with the concurrent expression of a destabilized mutant of γ D-crystallin. Initially identified in γ B-crystallin from a cataract mouse model [38], the I4F substitution has been studied extensively *in vitro* [39, 40]. The relatively minor destabilization and aggregation propensity of the mutant makes it ideal to investigate chaperone interactions with α -crystallin. Together, the results presented here reveal differences in the penetrance and severity of the phenotypes caused by the transgenic expression of the α -crystallin mutants. We demonstrate

that the more deleterious effects of R49C are the result of its driving the aggregation of lens proteins as predicted from the thermodynamic coupling model [11, 41].

Materials and methods

Zebrafish maintenance and breeding

AB wild-type strain zebrafish (*Danio rerio*) were used. The embryos were obtained by natural spawning and raised at 28.5°C on a 14/10 hour light/dark cycle in 0.3x Danieau water containing 0.003% PTU (w/v) to prevent pigment formation. Embryos were staged according to their ages (dpf; days post-fertilization). The following mutant and transgenic fish lines were used: *cryaa*^{vu532} [32], *cryaba*^{vu612}; *cryabb*^{vu613} [37], Tg(*cryaa*:*Rno.Cryaa_R49C*,*myl7*:*Cerulean*)^{vu615Tg}, Tg(*cryaa*:*Rno.Cryaa_R116C*,*myl7*:*Cerulean*)^{vu616Tg}, Tg(*cryaa*:*Mmu.Cryab_R120G*,*myl7*:*Cerulean*)^{vu617Tg} (this study), Tg(*cryaa*:*Gal4vp16*)^{mw46Tg}, Tg(*UAS*:*GFP*)^{kca33Tg} [42]. All animal procedures were verified and approved by the Vanderbilt University Institutional Animal Care and Use Committee.

Zebrafish transgenesis

To establish the transgenic zebrafish expressing rat (*Rno*) *Cryaa* gene (*Rno.Cryaa*) specifically in the lens, Tg(*cryaa*:*Rno.Cryaa*,*myl7*:*Cerulean*) was constructed by inserting mutated *Rno.Cryaa* cDNA (by site-mutagenesis; R49C and R116C) downstream of zebrafish *cryaa* promoter (1.2 kb) [43] in the pT2HBLR vector that was also contains *myl7* promoter-driven *Cerulean* as the selection marker (i.e. in the heart). Tol2 mediated transgenesis were performed as previously described [32] for the *Rno.Cryaa* (R49C and R116C) transgenes. The same protocol was followed for generating the mouse *cryab* R120G variant (*Mmu.Cryab_R120G*) transgene. Potential founder lines were selected by detecting cardiac *Cerulean* expression at 4dpf. At least two founder lines (F0) for each construct were screened and out-crossed to established stable F1 generations. Each F1 line was propagated and raised into F2 and F3 generations. The lens defects data collected were from F3 or F4 embryos, and similar penetrance of lens defects was observed in individual stable lines that express the same α -crystallin constructs.

Cell death assays

Embryos were fixed overnight at 4°C in 4% paraformaldehyde in PBS, dehydrated with 100% MeOH and stored in -20°C. The procedures of TUNEL staining were carried out following the manufacturer's suggested protocol (In Situ Cell Death Detection Kit, TMR red; Sigma-Aldrich #12156792910).

Microscopy and image processing

Lenses of live embryos in 0.3x Daneau water with PTU/tricane were analyzed by bright field microscopy (Zeiss Axiovert 200) at 4dpf and graded into three classes depending on the severity of lens defects as defined in our previous study [32]. Fluorescence images were taken with Zeiss AxioZoom.V16 microscope. Differential interference contrast (DIC) were performed by Zeiss LSM510 inverted confocal microscope with $\lambda_{em} = 488$ on 4dpf embryos which were embedded in 2.5% methylcellulose.

Statistics

The percentages of lens phenotype from multiple crosses (>2) for each experimental condition were averaged and reported as means \pm standard error (SE). For those only have two data

points, we reported the standard deviation (SD). Differences among comparing groups were analyzed by Student's *t*-test in Excel. Statistical significance was accepted when $p < 0.05$ (and marked as asterisk). Box plots were generated by BoxPlotR online software.

Results

Transgenic expression of α A-crystallin variants induce embryonic lens defects in zebrafish

To investigate the *in vivo* interactions between cataract-linked α A-crystallin mutants and lens chaperones in the context of the native environment of the lens fiber cells, we generated transgenic zebrafish lines that express the α A-crystallin mutants R49C and R116C (*Tg[cryaa:Rno.Cryaa_R49C]* and *Tg[cryaa:Rno.Cryaa_R116C]*; hereafter referred to as " α A-R49C" and " α A-R116C" for simplicity). Using zebrafish transgenesis protocols established previously [32], the two α A-crystallin variants were specifically expressed in the lens under the control of the zebrafish *cryaa* promoter with *myl7* promoter-driven Cerulean fluorescent protein in the heart as a convenient selection marker for transgenic animals.

Expression of both α A-crystallin variants led to various degrees of embryonic lens abnormalities that were readily visible starting at 3dpf, without affecting the overall morphology of the embryos (Fig 1A and 1B). The nature of these defects was similar to those previously described for α -crystallin deficient [32, 37] or γ D-crystallin mutant transgenic lines [33]. Defective lenses exhibited phenotypic features that were either spherical, shiny crystal-like droplets spread sporadically across the lens (minor defects), or frequent droplets covering a large fraction of the lens as well as occasional large irregular protuberances located in the center of the lens (major defects) (Fig 1B), all of which could lead to opacity and changes in light

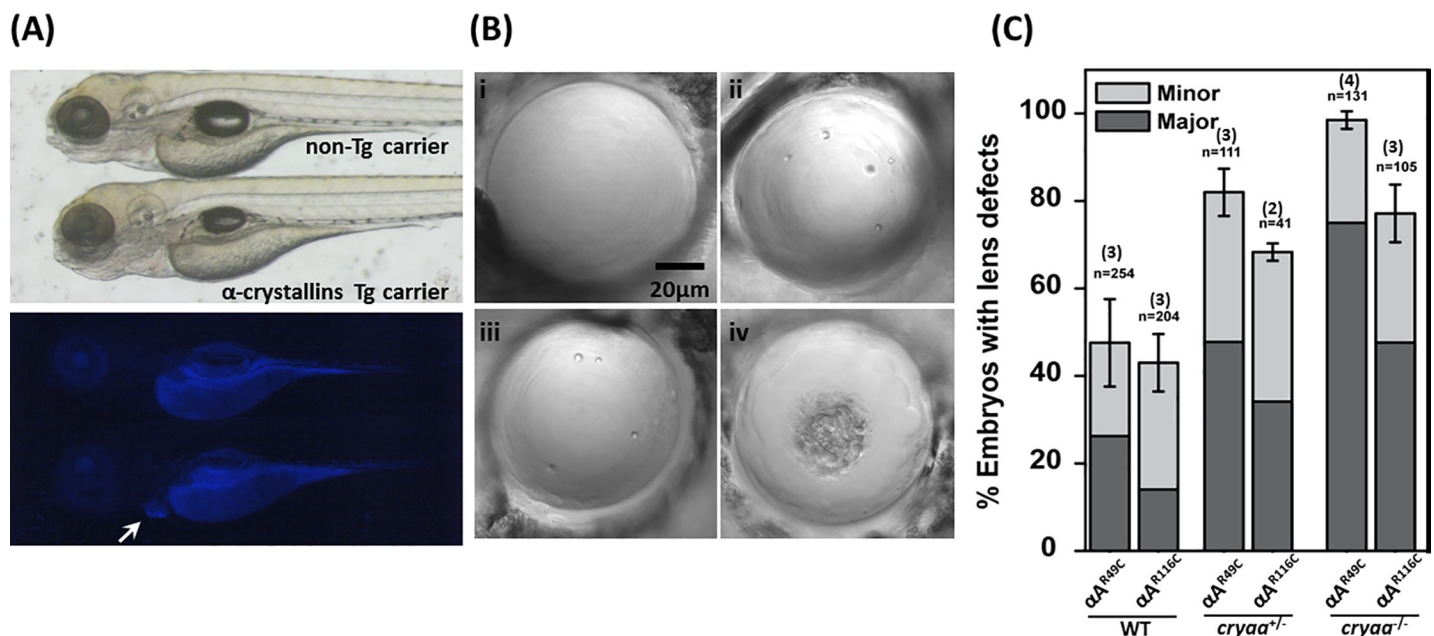


Fig 1. Transgenic expression of murine *Cryaa* mutants induced lens defects in 4dpf zebrafish embryos. (A) The lens-specific murine *Cryaa* transgenes displayed *Cerulean* marker in the heart. *Upper Panel*, DIC image. *Lower panel*, a white arrow marks the *Cerulean* marker in the heart. No overall morphology changes were observed in all transgenic carriers. (B) Representative DIC images of lenses from embryos expressing cataract-linked α A-crystallin mutants. The cataract phenotypes have been classified on the basis of the severity of defects. (i) WT, (ii, iii) minor defects (iv) major defects. (C) Embryos of lens-specific *Rno.Cryaa* transgenes (R49C and R116C mutations) displayed lens defects with various penetrance (scored at 4dpf). Removal of endogenous *cryaa* alleles exacerbated the lens defects. Error bars represented standard errors. Number of crosses is denoted in parentheses, n is the total number of screened embryos.

<https://doi.org/10.1371/journal.pone.0207540.g001>

scattering as previously reported [33]. For each α A-crystallin mutant, we screened a large number of embryos (see Fig 1C) and scored their lens phenotype based on the severity (Fig 1C). While the expression of both mutants led to a considerable fraction of embryos displaying lens defects, the data suggest a more deleterious consequence for the R49C mutation both in the penetrance and severity of the phenotype.

Genetic dosage of α A-crystallin determines the level of lens defects induced by the mutants

The R49C and R116C mutations of human α A-crystallin cause congenital cataracts in an autosomal dominant fashion, while only 40~50% of the embryos show lens defects in the transgenic fish lines expressing these mutant forms of α A-crystallin. The gene dosage of α A-crystallin has been shown to impact the penetrance and/or severity of lens phenotypes, as demonstrated earlier in *cryaa* zebrafish mutants [32] as well as the *Cryaa*-R49C knock-in mouse model [26], where the lenses from *Cryaa*-R49C homozygotes (equivalent of losing two copies of wild-type *Cryaa*) showed more severe lens opacity.

To investigate if the relatively moderate penetrance of lens defects was due to the expression of the endogenous zebrafish *cryaa* gene (i.e. wild-type) in these transgenic lines, we generated heterozygote α A-crystallin mutants. For this purpose, the *α A-R49C* and *α A-R116C* transgenic lines were crossed into *cryaa* null mutants [32] to create genetic conditions more closely mimicking the human autosomal dominant CRYAA mutations. The absence of one endogenous *cryaa* allele (i.e. *cryaa*^{+/-}), led to an increase in the percentage of lens defects from both α A-crystallin mutant transgenic lines, albeit not to 100% (Fig 1B). Absence of the other endogenous *cryaa* allele by backcrossing to generate α A-crystallin mutant transgenic lines under the *cryaa* null background (*cryaa*^{-/-}) further increased the percentage of embryos with lens defects approximating 100% penetrance for *α A-R49C* and near 80% for *α A-R116C*.

Because cell death has been implicated in cataract phenotypes, including radiation-induced cataracts, diabetic retinopathy-associated cataracts [44–46] as well as age-related cataract [47], we tested for apoptotic cell death in the transgenic lines. TUNEL assay (Fig 2) did not show evidence of elevated apoptosis in the embryonic lens carrying α A-crystallin mutant transgenes when compared to WT. Therefore, cell death by apoptosis does not seem to play a major role in the embryonic lens defects in the α A-crystallin zebrafish transgenes, a result which differs from mouse α A-crystallin knock-in and transgenic models [24, 26] where increase of cell death were reported in the postnatal lens.

α A-R49C but not R116C increases the phenotype penetrance of a destabilized γ -crystallin mutant

The model of Koteiche and Mchaourab predicts that R49C and R116C would act to bind native lens proteins driving unfolding and aggregation [11, 48] and leading to formation of large particulates that scatter light. To test this model, we co-expressed each of the mutants with the human γ D-crystallin variant I4F [33]. The I4F substitution reduces the free energy of unfolding reflecting a lower stability of the N-terminal domain [39]. In addition, the mutant exhibits a slow aggregation susceptibility *in vitro* [40]. Transgenic expression of γ D-crystallin I4F mutant by itself resulted in moderate frequency (~30%) of major lens defects (*γ D-I4F*; Fig 3), consistent with our previous study [33]. We focused on the major defects because of their direct correlation to aggregation of γ D-crystallin I4F (see below).

Co-expression of the *α A-R49C* transgene with *γ D-I4F* (i.e. *α A-R49C*; *γ D-I4F*) led to a synergistic effect significantly ($p < 0.05$) increasing the percentage of major lens defects. In contrast, co-expression of *α A-R116C* did not significantly change the severity or penetrance of the lens

(A)



(B)

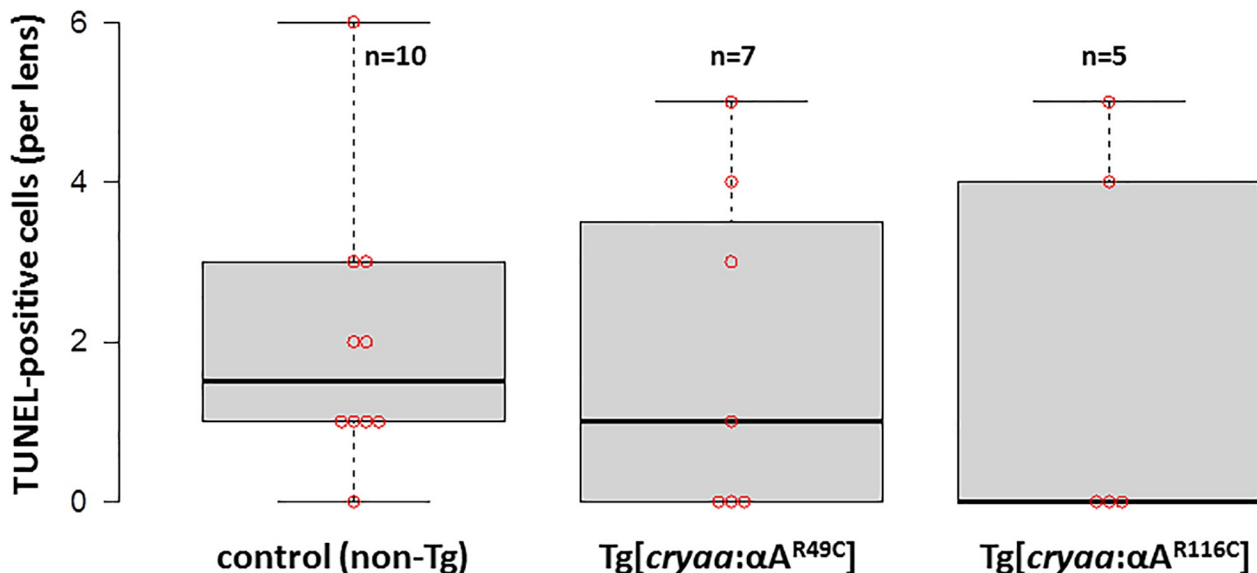


Fig 2. Apoptotic cell death was not induced by transgenic expression of murine *Cryaa* mutants. TUNEL staining (A), embryos of *Tg(cryaa:Rno.Cryaa_R49C)* and *Tg(cryaa:Rno.Cryaa_R116C)* did not show increase of apoptosis in the lens when compared to non-transgenic (WT) siblings (B). Center black lines show the medians; box limits indicate the 25th and 75th percentiles as determined by R software; whiskers extend 1.5 times the interquartile range from the 25th and 75th percentiles. Individual sample points are shown by red circle.

<https://doi.org/10.1371/journal.pone.0207540.g002>

defects (αA -R116C; γD -I4F), which remained comparable with single transgenic embryos (γD -I4F) (Fig 3).

Expression of αA -R49C increases the susceptibility of destabilized γD -crystallin to aggregation

In a previous study, we demonstrated that the penetrance of lens defects due to the expression of destabilized γD -crystallin mutant proteins strongly correlated with their susceptibility to form aggregates in the zebrafish lens [33]. Thus, the enhanced lens defects observed in the double transgenic embryos (Fig 3; αA -R49C; γD -I4F) could result from increased aggregation of γD -I4F when the αA -R49C transgene was co-expressed.

We directly tested this model utilizing a similar experimental approach with the Gal4/UAS expression system to facilitate mosaic analysis (Fig 4A). γD -crystallin mutant was tagged by

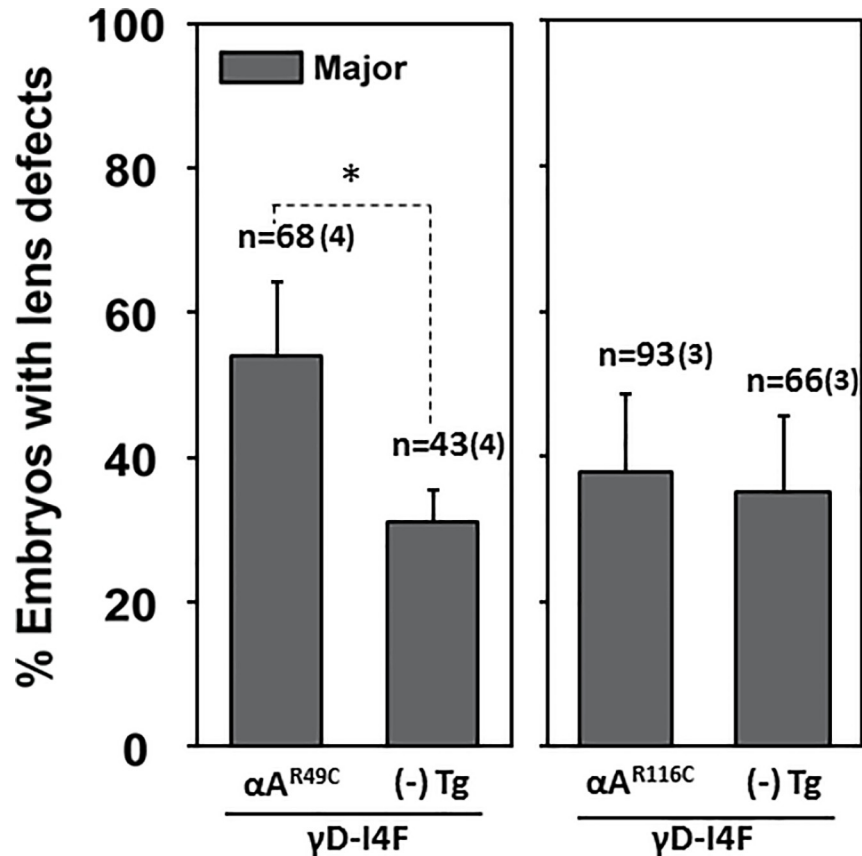


Fig 3. Synergistic effects on embryonic lens defects were selectively observed in transgenic co-expression of the human *CRYGD* mutant and murine *Cryaa* mutants. Compared to the siblings carrying single transgene, *Tg(cryaa: Hsa.CRYGD_I4F)*, double transgenic embryos at 4dpf exhibited enhanced penetrance of lens defects when *Tg(cryaa: Rno.Cryaa_R49C)* was co-expressed, but not *Tg(cryaa:Rno.Cryaa_R116C)*. Error bars represented standard errors. Number of crosses is denoted in parentheses.

<https://doi.org/10.1371/journal.pone.0207540.g003>

red fluorescent protein and the aggregation was detected by the observation of fluorescent punctates as demonstrated previously [33]. By comparing the percentage of fluorescent punctate formation (i.e. mCherry-tagged γ D-I4F) between transgenic carriers and non-transgenic embryos, we observed a significant difference between αA -R49C and αA -R116C transgenes in inducing γ D-crystallin aggregation (Fig 4B). In the presence of the αA -R49C transgene, the percentage of embryos with fluorescent punctates, which reflects γ D-crystallin aggregation, was higher by about 15~20% (Left panel); while no apparent difference was observed regardless of the expression of αA -R116C (Right panel). As expected, the phenotype penetrance of αA -R49C is increased in the absence of endogenous αA -crystallin.

A higher percentage of embryos displaying γ D-crystallin aggregation (manifested by fluorescent punctate formation) was observed for the non-transgenic embryos from the αA -R116C crosses compared to the ones from the αA -R49C crosses (Fig 4B). A number of potential reasons could contribute to this difference. First, the stochastic nature of mosaic analysis, where the mCherry-tagged γ D-crystallin cDNA constructs were randomly distributed in the lens fiber cells by microinjection, probably led to different expression/distribution of γ D-crystallin, even though the same nominal amount of DNA was injected into each 1-cell zygote. Consistent with this conjecture, a wide-range of positive F0 carriers was reported in the context of zebrafish transgenesis [49]. Second and of critical importance is the underappreciated

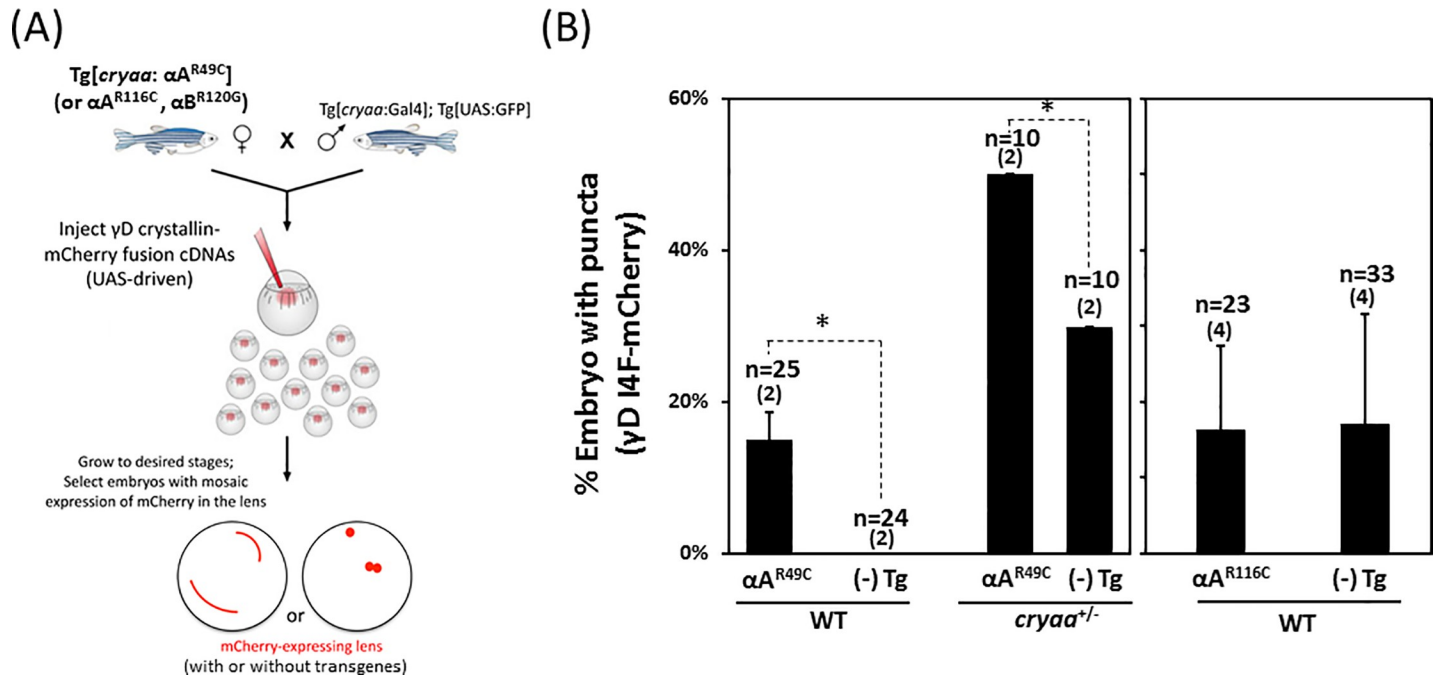


Fig 4. Differential modulation of γD -crystallin protein aggregation by transgenes of murine *Cryaa* mutants. (A) Schematic of the experiment utilizing the Gal4/UAS targeted gene expression system. Double transgenic line, $Tg[crystallin:Gal4]; Tg[UAS:GFP]$, were outcrossed to either $\alpha A-R49C$, $crystallin^{-/-}; \alpha A-R49C$, $\alpha A-R116C$ (shown in Fig 4B) or $\alpha B-R120G$ (shown in Fig 5B) transgenic lines. Fertilized zygotes were injected with tol2 mRNA and UAS responder Tol2 constructs expressing fluorescently tagged human γD -crystallin (*Hsa.CRYGD_I4F-mCherry*). Embryos possessing lens fiber cells positive for mCherry mosaic expression were selected and imaged at 4dpf. (B) The percentage of embryos showing γD -crystallin_I4F-mCherry punctuates in the lens were significantly increased when $Tg[crystallin:Rno.Cryaa_{R49C}]$ was co-expressed, but not with $Tg[crystallin:Rno.Cryaa_{R116C}]$. Error bars represented standard deviations in $\alpha A-R49C$ crosses (left panel,) and standard errors in $\alpha A-R116C$ crosses (right panel). Number of crosses is denoted in parentheses.

<https://doi.org/10.1371/journal.pone.0207540.g004>

phenomenon of cross-generational effects of genetic modifiers [50], which was also suggested to account for variations in lens defects severity in the progeny of $crystallin^{+/-}$ adult lines in a previous study [32]. The adult transgenic $\alpha A-R116C$ and $\alpha A-R49C$ fish lines used here were neither phenotypically screened/selected before raised to adulthood, nor restricted for any particular sex (i.e. random usage of male and female fishes). Thus, the zygotes from $\alpha A-R116C$ and $\alpha A-R49C$ crosses may possess intrinsically different proteostasis capacity inherited from their parents, which would manifest as a difference in the basal level of protein aggregation.

Expression of murine αB -crystallin R120G mutant induces zebrafish lens defects but does not promote γD -crystallin aggregation

αB -crystallin is a molecular chaperone involved in the cell response to stress in various tissues (see reviews in [51, 52]). Loss-of-function studies demonstrated that αB -crystallin is critical in maintaining lens proteostasis [37], and several missense mutations in human αB -crystallin gene are linked to hereditary cataracts, including P20S [53] and D140N [54]. The most-studied mutation, R120G, resides within the α -crystallin domain and is associated with desmin-related myopathy [20, 55].

Because αB -crystallin R120 is homologous to αA -crystallin R116 and the two mutations (R120G and R116C) have similar properties *in vitro*, we generated a transgenic line expressing the αB -crystallin R120G mutant specifically in the lens ($\alpha B-R120G$). As expected $\alpha B-R120G$ induced lens defects with a moderate penetrance but the severity of lens phenotypes was mostly of the minor class (Fig 5A). Reducing endogenous αB -crystallin levels by crossing

αB -R120G into zebrafish αB -crystallin null mutants (*cryaba*^{-/-}; *cryabb*^{-/-}) [37] led to significant enhancement of lens defects in both penetrance and severity (Fig 5A) compared to αB -crystallin null mutants alone [37]. This is similar to the increase in penetrance and severity of lens defects in the absence of endogenous αA -crystallin.

If the nature of the substitution- i.e. glycine versus cysteine is not critical for the interaction with γD -crystallin, then the results of αA -R116C in Fig 4 predicts that αB -R120G would have a minimal effect on the propensity of γD -crystallin aggregation. Indeed, transgenic expression of αB -R120G did not significantly increase the percentage of embryos displaying γD -I4F aggregation when compared to non-transgenic siblings (Fig 5B). Together with the results from the αA -crystallin transgenic lines, this finding suggests that the increase in the penetrance of γD -crystallin aggregation phenotype induced by R49C co-expression is directly related to the position of R49 in the primary sequence.

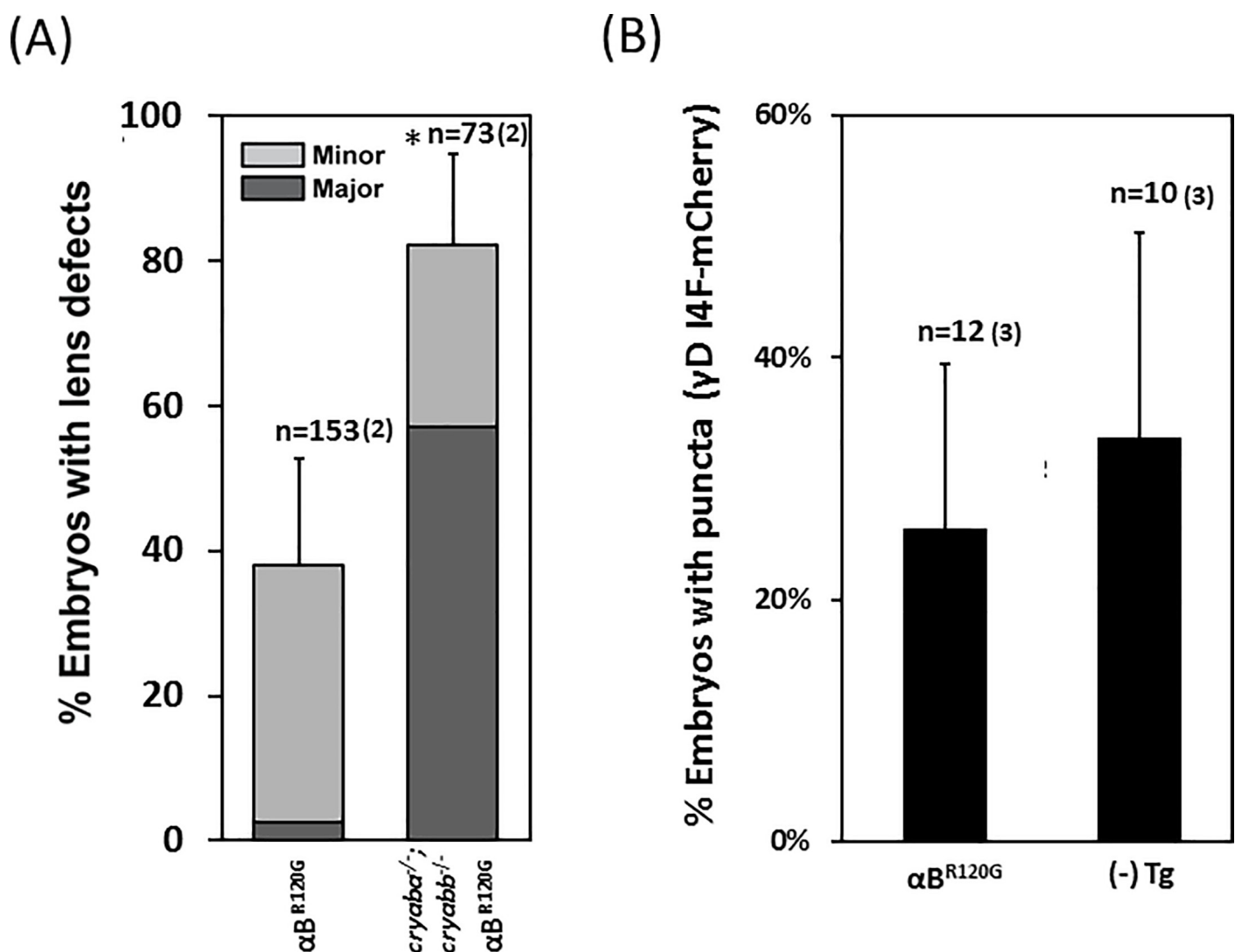


Fig 5. The effects on γD -crystallin protein aggregation by transgenes of murine αB -crystallin R120G mutant. (A) Transgenic expression of mouse *Cryab* R120G mutant induced lens defects in 4dpf zebrafish embryos, and lens defects were significantly exacerbated in the background of αB -crystallin null (*cryaba*^{-/-}; *cryabb*^{-/-}). (B) The percentage of embryos showing mCherry-tagged γD -I4F punctates in the lens were not changed when co-expressed with *Tg(cryaa:Mmu.Cryab_R120G)*. Error bars represented standard deviations in (A) and standard errors in (B). Number of crosses is denoted in parentheses.

<https://doi.org/10.1371/journal.pone.0207540.g005>

Discussion

The work reported here takes advantage of the power of zebrafish as a model organism to carry out the first direct comparison between cataract-linked mutants of α A-crystallin in a similar genetic background. R49C and R116C are two human autosomal-dominant mutations that have been associated with a wide range of effects on the structure and function of α A-crystallin. Similar to mouse models, expression of these mutants in the zebrafish lens leads to lens defects that have been previously demonstrated to cause increased light scattering [32, 33]. While the absence of one copy of the WT protein (i.e. endogenous allele) accentuates the penetrance and severity of the phenotype, the R49C mutation was consistently more deleterious than the R116C mutation. We linked the differential effects of the two mutants to the R49C being more effective in inducing protein aggregation. These mutants have similar chaperone properties as deduced from *in vitro* binding studies to the model client protein T4L [11]. Thus, our findings highlight the importance of *in vivo* investigation in validating mechanistic models.

How does co-expression of α A-R49C drive γ D-I4F aggregation? Our thermodynamic coupling model [11] predicts that an increase in the apparent affinity of the chaperone to the unfolded state of the client protein would drive unfolding of the latter by simple mass action laws, i.e. the folding equilibrium is shifted towards the unfolded state as a result of it being depleted by binding to the chaperone. In the double transgenic line, the interaction with the γ D-crystallin mutant is expected to be exclusive to the R49C mutant because of its higher affinity to γ D-crystallin [39]. Therefore, if the level of expression of the two proteins is similar, a reasonable assumption given that both are transgenically driven by the same *cryaa* promoter with a single genomic insertion [33], we predict that the aggregation of γ D-I4F involves the formation of 1 to 1 complexes with the R49C. Experiments are underway to test this conclusion.

In addition to enhanced binding affinity, R49C, but not R116C, has been shown to undergo disulfide cross-linking at the mutation site [41] suggesting that the location of the cysteine is critical. In studies of binding to the client protein β B1-crystallin, formation of an α A-R49C dimer involving a mixed α/β -crystallin intermediate was observed [41]. This dimer was strictly dependent on the labeling of β B1 at a single cysteine by a disulfide-linked fluorescent probe, suggesting that the formation of chaperone/client protein complex is an intermediate step [41]. Because human γ -crystallins contain multiple cysteines, we predict that the formation of the complex with R49C is stabilized by disulfide cross-links. Previous studies have shown that the R49C mutation in human γ D-crystallin increases the propensity of intermolecular disulfide bond formation [56, 57]. Importantly, in the homozygote knock-in R49C mouse line, the mutant α A-crystallin was reported to be disulfide cross-linked although the construct contained a second cysteine, which could lead to different types of covalent dimers. Consistent with our conclusion that disulfide cross-linking is the primary factor in the deleterious effect of the R49C mutation, the α B-crystallin R120G mutant did not promote the aggregation of γ D-I4F.

Finally, a critical parameter typically missing *in vitro* is molecular crowding, which in lens fiber cells is predicted to substantially alter the thermodynamics of molecular interactions. Not only does the excluded volume effect, due to crowding, stabilize the folded states of client proteins but it is also predicted to affect the subunit exchange of the α -crystallins [58, 59]. Equilibrium dissociation of α -crystallins is a mechanism of chaperone activation [23]. In this context, it is notable that the two mutations (R49C, and R116C) have profoundly different effects on the organization of the oligomeric structure [11]. Our finding of distinctive phenotypic effects of the two mutants in a model organism emphasizes the necessity of challenging mechanistic

conclusions obtained *in vitro* and highlights the role of cellular context in shaping chaperone interactions with native client proteins.

Acknowledgments

We thank Dr. Derek Claxton for critical reading of the manuscript and Abigail Poff for technical assistance.

Author Contributions

Conceptualization: Shu-Yu Wu, Hassane S. Mchaourab.

Data curation: Shu-Yu Wu, Ping Zou.

Formal analysis: Shu-Yu Wu.

Funding acquisition: Hassane S. Mchaourab.

Investigation: Shu-Yu Wu.

Resources: Ping Zou, Sanjay Mishra.

Supervision: Hassane S. Mchaourab.

Writing – original draft: Shu-Yu Wu, Hassane S. Mchaourab.

Writing – review & editing: Shu-Yu Wu, Hassane S. Mchaourab.

References

1. Benedek GB. Cataract as a protein condensation disease: the Proctor Lecture. *Investigative ophthalmology & visual science*. 1997; 38(10):1911–21.
2. Bloemendal H, de Jong W, Jaenicke R, Lubsen NH, Slingsby C, Tardieu A. Ageing and vision: structure, stability and function of lens crystallins. *Progress in Biophysics & Molecular Biology*. 2004; 86(3):407–85. <https://doi.org/10.1016/j.pbiomolbio.2003.11.012> PMID: 15302206.
3. Sharma KK, Santhoshkumar P. Lens aging: effects of crystallins. *Biochimica et biophysica acta*. 2009; 1790(10):1095–108. Epub 2009/05/26. <https://doi.org/10.1016/j.bbagen.2009.05.008> PMID: 19463898; PubMed Central PMCID: PMC2743770.
4. Clark AR, Lubsen NH, Slingsby C. sHSP in the eye lens: crystallin mutations, cataract and proteostasis. *Int J Biochem Cell Biol*. 2012; 44(10):1687–97. <https://doi.org/10.1016/j.biocel.2012.02.015> PMID: 22405853.
5. Andley UP. Crystallins in the eye: Function and pathology. *Progress in Retinal & Eye Research*. 2007; 26(1):78–98. <https://doi.org/10.1016/j.preteyeres.2006.10.003> PMID: 17166758.
6. Truscott RJW. Age-related nuclear cataract-oxidation is the key. *Experimental eye research*. 2005; 80(5):709–25. <https://doi.org/10.1016/j.exer.2004.12.007> PMID: 15862178.
7. Hanson SR, Hasan A, Smith DL, Smith JB. The major *in vivo* modifications of the human water-insoluble lens crystallins are disulfide bonds, deamidation, methionine oxidation and backbone cleavage. *Experimental eye research*. 2000; 71(2):195–207. <https://doi.org/10.1006/exer.2000.0868> PMID: 10930324.
8. Lampi KJ, Ma Z, Hanson SR, Azuma M, Shih M, Shearer TR, et al. Age-related changes in human lens crystallins identified by two-dimensional electrophoresis and mass spectrometry. *Experimental eye research*. 1998; 67(1):31–43. <https://doi.org/10.1006/exer.1998.0481> PMID: 9702176
9. Claxton DP, Zou P, McHaourab HS. Structure and orientation of T4 lysozyme bound to the small heat shock protein α -crystallin. *Journal of molecular biology*. 2008; 375(4):1026–39. <https://doi.org/10.1016/j.jmb.2007.11.014> PMID: 18062989.
10. Shashidharamurthy R, Koteiche HA, Dong J, McHaourab HS. Mechanism of chaperone function in small heat shock proteins: dissociation of the HSP27 oligomer is required for recognition and binding of destabilized T4 lysozyme. *The Journal of biological chemistry*. 2005; 280(7):5281–9. <https://doi.org/10.1074/jbc.M407236200> PMID: 15542604.

11. Koteiche HA, McHaourab HS. Mechanism of a hereditary cataract phenotype. Mutations in alphaA-crystallin activate substrate binding. *The Journal of biological chemistry*. 2006; 281(20):14273–9. Epub 2006/03/15. <https://doi.org/10.1074/jbc.M512938200> PMID: 16531622.
12. Koteiche HA, McHaourab HS. Mechanism of chaperone function in small heat-shock proteins. Phosphorylation-induced activation of two-mode binding in alphaB-crystallin. *Journal of Biological Chemistry*. 2003; 278(12):10361–7. <https://doi.org/10.1074/jbc.M211851200> PMID: 12529319
13. Mchaourab HS, Dodson EK, Koteiche HA. Mechanism of Chaperone Function in Small Heat-Shock Proteins. Two-Mode Binding of the Excited States of T4 Lysozyme Mutants by α A-Crystallin. *Journal of Biological Chemistry*. 2002; 277:40557–66. <https://doi.org/10.1074/jbc.M206250200> PMID: 12189146
14. Benesch JL, Ayoub M, Robinson CV, Aquilina JA. Small heat shock protein activity is regulated by variable oligomeric substructure. *The Journal of biological chemistry*. 2008; 283(42):28513–7. Epub 2008/08/21. <https://doi.org/10.1074/jbc.M804729200> PMID: 18713743; PubMed Central PMCID: PMC2661405.
15. Sharma KK, Kaur H, Kester K. Functional elements in molecular chaperone alpha-crystallin: identification of binding sites in alpha B-crystallin. *Biochemical and biophysical research communications*. 1997; 239(1):217–22. Epub 1997/11/05. <https://doi.org/10.1006/bbrc.1997.7460> PMID: 9345298.
16. Peschek J, Braun N, Rohrberg J, Back KC, Kriehuber T, Kastenmuller A, et al. Regulated structural transitions unleash the chaperone activity of alphaB-crystallin. *Proceedings of the National Academy of Sciences of the United States of America*. 2013; 110(40):E3780–9. Epub 2013/09/18. <https://doi.org/10.1073/pnas.1308898110> PMID: 24043785; PubMed Central PMCID: PMC3791731.
17. Cox D, Selig E, Griffin MD, Carver JA, Ecroyd H. Small Heat-shock Proteins Prevent alpha-Synuclein Aggregation via Transient Interactions and Their Efficacy Is Affected by the Rate of Aggregation. *The Journal of biological chemistry*. 2016; 291(43):22618–29. <https://doi.org/10.1074/jbc.M116.739250> PMID: 27587396; PubMed Central PMCID: PMC45077198.
18. Horwitz J. Alpha-crystallin. *Experimental Eye Research*. 2003; 76(2):145–53. PMID: 12565801
19. Cobb BA, Petrash JM. Structural and functional changes in the alpha A-crystallin R116C mutant in hereditary cataracts. *Biochemistry*. 2000; 39(51):15791–8. PMID: 11123904; PubMed Central PMCID: PMC2902970.
20. Bova MP, Yaron O, Huang Q, Ding L, Haley DA, Stewart PL, et al. Mutation R120G in alphaB-crystallin, which is linked to a desmin-related myopathy, results in an irregular structure and defective chaperone-like function. *Proceedings of the National Academy of Sciences of the United States of America*. 1999; 96(11):6137–42. PMID: 10339554; PubMed Central PMCID: PMC26848.
21. Simon S, Michiel M, Skouri-Panet F, Lechaire JP, Vicart P, Tardieu A. Residue R120 is essential for the quaternary structure and functional integrity of human alphaB-crystallin. *Biochemistry*. 2007; 46(33):9605–14. <https://doi.org/10.1021/bi7003125> PMID: 17655279.
22. Kore R, Hedges RA, Oonthonpan L, Santhoshkumar P, Sharma KK, Abraham EC. Quaternary structural parameters of the congenital cataract causing mutants of alphaA-crystallin. *Mol Cell Biochem*. 2012; 362(1–2):93–102. <https://doi.org/10.1007/s11010-011-1131-8> PMID: 22045060; PubMed Central PMCID: PMC3788686.
23. McHaourab HS, Godar JA, Stewart PL. Structure and mechanism of protein stability sensors: chaperone activity of small heat shock proteins. *Biochemistry*. 2009; 48(18):3828–37. <https://doi.org/10.1021/bi900212j> PMID: 19323523.
24. Hsu CD, Kymes S, Petrash JM. A transgenic mouse model for human autosomal dominant cataract. *Investigative ophthalmology & visual science*. 2006; 47(5):2036–44. <https://doi.org/10.1167/iovs.05-0524> PMID: 16639013; PubMed Central PMCID: PMC1855087.
25. Andley UP, Hamilton PD, Ravi N, Wehl CC. A knock-in mouse model for the R120G mutation of alphaB-crystallin recapitulates human hereditary myopathy and cataracts. *PloS one*. 2011; 6(3):e17671. <https://doi.org/10.1371/journal.pone.0017671> PMID: 21445271; PubMed Central PMCID: PMC3060869.
26. Xi JH, Bai F, Gross J, Townsend RR, Menko AS, Andley UP. Mechanism of small heat shock protein function in vivo: a knock-in mouse model demonstrates that the R49C mutation in alpha A-crystallin enhances protein insolubility and cell death. *The Journal of biological chemistry*. 2008; 283(9):5801–14. <https://doi.org/10.1074/jbc.M708704200> PMID: 18056999.
27. Andley UP, Tycksen E, McGlasson-Naumann BN, Hamilton PD. Probing the changes in gene expression due to alpha-crystallin mutations in mouse models of hereditary human cataract. *PloS one*. 2018; 13(1):e0190817. <https://doi.org/10.1371/journal.pone.0190817> PMID: 29338044; PubMed Central PMCID: PMC5770019.
28. Fadool JM, Dowling JE. Zebrafish: a model system for the study of eye genetics. *Progress in Retinal & Eye Research*. 2008; 27(1):89–110.

29. Greiling TM, Clark JI. New insights into the mechanism of lens development using zebra fish. *Int Rev Cell Mol Biol.* 2012; 296:1–61. <https://doi.org/10.1016/B978-0-12-394307-1.00001-1> PMID: 22559937.
30. Goishi K, Shimizu A, Najarro G, Watanabe S, Rogers R, Zon LI, et al. AlphaA-crystallin expression prevents gamma-crystallin insolubility and cataract formation in the zebrafish cloche mutant lens. *Development.* 2006; 133(13):2585–93. <https://doi.org/10.1242/dev.02424> PMID: 16728471
31. Greiling TM, Clark JI. Early lens development in the zebrafish: a three-dimensional time-lapse analysis. *Developmental Dynamics.* 2009; 238(9):2254–65. <https://doi.org/10.1002/dvdy.21997> PMID: 19504455
32. Zou P, Wu SY, Koteiche HA, Mishra S, Levic DS, Knapik E, et al. A conserved role of alphaA-crystallin in the development of the zebrafish embryonic lens. *Experimental eye research.* 2015; 138:104–13. Epub 2015/07/08. <https://doi.org/10.1016/j.exer.2015.07.001> PMID: 26149094; PubMed Central PMCID: PMC4638411.
33. Wu SY, Zou P, Fuller AW, Mishra S, Wang Z, Schey KL, et al. Expression of Cataract-linked gamma-Crystallin Variants in Zebrafish Reveals a Proteostasis Network That Senses Protein Stability. *The Journal of biological chemistry.* 2016; 291(49):25387–97. <https://doi.org/10.1074/jbc.M116.749606> PMID: 27770023; PubMed Central PMCID: PMC5207241.
34. Posner M, Skiba J, Brown M, Liang JO, Nussbaum J, Prior H. Loss of the small heat shock protein alphaA-crystallin does not lead to detectable defects in early zebrafish lens development. *Experimental eye research.* 2013; 116:227–33. <https://doi.org/10.1016/j.exer.2013.09.007> PMID: 24076322.
35. Soules KA, Link BA. Morphogenesis of the anterior segment in the zebrafish eye. *BMC Developmental Biology.* 2005; 5:12. <https://doi.org/10.1186/1471-213X-5-12> PMID: 15985175
36. Posner M, Hawke M, Lacava C, Prince CJ, Bellanco NR, Corbin RW. A proteome map of the zebrafish (*Danio rerio*) lens reveals similarities between zebrafish and mammalian crystallin expression. *Molecular vision.* 2008; 14:806–14. PMID: 18449354
37. Mishra S, Wu SY, Fuller AW, Wang Z, Rose KL, Schey KL, et al. Loss of alphaB-crystallin function in zebrafish reveals critical roles in the development of the lens and stress resistance of the heart. *The Journal of biological chemistry.* 2018; 293(2):740–53. <https://doi.org/10.1074/jbc.M117.808634> PMID: 29162721; PubMed Central PMCID: PMC5767876.
38. Liu H, Du X, Wang M, Huang Q, Ding L, McDonald HW, et al. Crystallin {gamma}B-14F mutant protein binds to {alpha}-crystallin and affects lens transparency. *Journal of Biological Chemistry.* 2005; 280(26):25071–8. <https://doi.org/10.1074/jbc.M502490200> PMID: 15878859.
39. Mishra S, Stein RA, McHaourab HS. Cataract-linked gammaD-crystallin mutants have weak affinity to lens chaperones alpha-crystallins. *FEBS Letters.* 2012; 586(4):330–6. <https://doi.org/10.1016/j.febslet.2012.01.019> PMID: 22289178
40. Moreau KL, King JA. Cataract-causing defect of a mutant gamma-crystallin proceeds through an aggregation pathway which bypasses recognition by the alpha-crystallin chaperone. *PloS one.* 2012; 7(5): e37256. Epub 2012/06/02. <https://doi.org/10.1371/journal.pone.0037256> PMID: 22655036; PubMed Central PMCID: PMC3360035.
41. Kumar MS, Koteiche HA, Claxton DP, McHaourab HS. Disulfide cross-links in the interaction of a cataract-linked alphaA-crystallin mutant with betaB1-crystallin. *FEBS Lett.* 2009; 583(1):175–9. <https://doi.org/10.1016/j.febslet.2008.11.047> PMID: 19071118.
42. Hayes JM, Hartsock A, Clark BS, Napier HR, Link BA, Gross JM. Integrin alpha5/fibronectin1 and focal adhesion kinase are required for lens fiber morphogenesis in zebrafish. *Molecular biology of the cell.* 2012; 23(24):4725–38. Epub 2012/10/26. <https://doi.org/10.1091/mbc.E12-09-0672> PMID: 23097490; PubMed Central PMCID: PMC3521681.
43. Kurita R, Sagara H, Aoki Y, Link BA, Arai K, Watanabe S. Suppression of lens growth by alphaA-crystallin promoter-driven expression of diphtheria toxin results in disruption of retinal cell organization in zebrafish. *Developmental biology.* 2003; 255(1):113–27. Epub 2003/03/06. PMID: 12618137.
44. Li WC, Kuszak JR, Dunn K, Wang RR, Ma W, Wang GM, et al. Lens epithelial cell apoptosis appears to be a common cellular basis for non-congenital cataract development in humans and animals. *The Journal of cell biology.* 1995; 130(1):169–81. Epub 1995/07/01. PMID: 7790371; PubMed Central PMCID: PMC2120521.
45. Zhang L, Yan Q, Liu JP, Zou LJ, Liu J, Sun S, et al. Apoptosis: its functions and control in the ocular lens. *Current molecular medicine.* 2010; 10(9):864–75. Epub 2010/11/26. PMID: 21091420.
46. Okamura N, Ito Y, Shibata MA, Ikeda T, Otsuki Y. Fas-mediated apoptosis in human lens epithelial cells of cataracts associated with diabetic retinopathy. *Medical electron microscopy: official journal of the Clinical Electron Microscopy Society of Japan.* 2002; 35(4):234–41. Epub 2003/03/27. <https://doi.org/10.1007/s007950200027> PMID: 12658358.

47. Harocopos GJ, Alvares KM, Kolker AE, Beebe DC. Human age-related cataract and lens epithelial cell death. *Investigative ophthalmology & visual science*. 1998; 39(13):2696–706. Epub 1998/12/18. PMID: [9856780](#).
48. Berengian AR, Bova MP, McHaourab HS. Structure and function of the conserved domain in alphaA-crystallin. Site-directed spin labeling identifies a beta-strand located near a subunit interface. *Biochemistry*. 1997; 36(33):9951–7. <https://doi.org/10.1021/bi9712347> PMID: [9296605](#).
49. Kawakami K. Transgenesis and gene trap methods in zebrafish by using the Tol2 transposable element. *Methods Cell Biol*. 2004; 77:201–22. PMID: [15602913](#).
50. Rakyan V, Whitelaw E. Transgenerational epigenetic inheritance. *Curr Biol*. 2003; 13(1):R6. PMID: [12526754](#).
51. Boelens WC. Cell biological roles of alphaB-crystallin. *Progress in biophysics and molecular biology*. 2014; 115(1):3–10. Epub 2014/03/01. <https://doi.org/10.1016/j.pbiomolbio.2014.02.005> PMID: [24576798](#).
52. Bakthisaran R, Akula KK, Tangirala R, Rao Ch M. Phosphorylation of alphaB-crystallin: Role in stress, aging and patho-physiological conditions. *Biochimica et biophysica acta*. 2016; 1860(1 Pt B):167–82. <https://doi.org/10.1016/j.bbagen.2015.09.017> PMID: [26415747](#).
53. Liu M, Ke T, Wang Z, Yang Q, Chang W, Jiang F, et al. Identification of a CRYAB mutation associated with autosomal dominant posterior polar cataract in a Chinese family. *Investigative ophthalmology & visual science*. 2006; 47(8):3461–6. <https://doi.org/10.1167/iovs.05-1438> PMID: [16877416](#).
54. Liu Y, Zhang X, Luo L, Wu M, Zeng R, Cheng G, et al. A novel alphaB-crystallin mutation associated with autosomal dominant congenital lamellar cataract. *Investigative ophthalmology & visual science*. 2006; 47(3):1069–75. <https://doi.org/10.1167/iovs.05-1004> PMID: [16505043](#); PubMed Central PMCID: PMC2078606.
55. Vicart P, Caron A, Guicheney P, Li Z, Prevost MC, Faure A, et al. A missense mutation in the alphaB-crystallin chaperone gene causes a desmin-related myopathy. *Nature genetics*. 1998; 20(1):92–5. Epub 1998/09/10. <https://doi.org/10.1038/1765> PMID: [9731540](#).
56. Pande A, Pande J, Asherie N, Lomakin A, Ogun O, King JA, et al. Molecular basis of a progressive juvenile-onset hereditary cataract. *Proceedings of the National Academy of Sciences of the United States of America*. 2000; 97(5):1993–8. <https://doi.org/10.1073/pnas.040554397> PMID: [10688888](#); PubMed Central PMCID: PMC215742.
57. Pande A, Gillot D, Pande J. The cataract-associated R14C mutant of human gamma D-crystallin shows a variety of intermolecular disulfide cross-links: a Raman spectroscopic study. *Biochemistry*. 2009; 48(22):4937–45. <https://doi.org/10.1021/bi9004182> PMID: [19382745](#); PubMed Central PMCID: PMC2707855.
58. van den Berg B, Ellis RJ, Dobson CM. Effects of macromolecular crowding on protein folding and aggregation. *EMBO Journal*. 1999; 18(24):6927–33. <https://doi.org/10.1093/emboj/18.24.6927> PMID: [10601015](#)
59. van den Berg B, Wain R, Dobson CM, Ellis RJ. Macromolecular crowding perturbs protein refolding kinetics: implications for folding inside the cell. *EMBO Journal*. 2000; 19(15):3870–5. <https://doi.org/10.1093/emboj/19.15.3870> PMID: [10921869](#)